OPEN ACCESS
Journal of Innovative Optical Health Sciences
Vol. 17, No. 2 (2024) 2350018 (11 pages)

DOI: 10.1142/S1793545823500189

World Scientific
www.worldscientific.com

MACS-W: A modified optical clearing agent for imaging 3D cell cultures

Xiang Zhong[*,†], Chao Gao[*,†], Hui Li[*,†], Yuening He[*,†], Peng Fei[†,‡], Zaozao Chen[§,¶], Zhongze Gu[§,¶], Dan Zhu[*,†] and Tingting Yu[*,†,‖]

[*]*Britton Chance Center for Biomedical Photonics – MoE Key Laboratory for Biomedical Photonics*
Huazhong University of Science and Technology
Wuhan, Hubei 430074, P. R. China

[†]*Wuhan National Laboratory for Optoelectronics – Advanced Biomedical Imaging Facility*
Huazhong University of Science and Technology
Wuhan, Hubei 430074, P. R. China

[‡]*School of Optical and Electronic Information*
Huazhong University of Science and Technology
Wuhan, Hubei 430074, P. R. China

[§]*State Key Laboratory of Bioelectronics*
School of Biological Science and Medical Engineering
Southeast University, Nanjing, Jiangsu 210096, P. R. China

[¶]*Institute of Biomaterials and Medical Devices*
Southeast University, Suzhou
Jiangsu 215163, P. R. China
[‖]*yutingting@hust.edu.cn*

Received 30 March 2023
Accepted 6 June 2023
Published 12 July 2023

Three-dimensional (3D) cell cultures have contributed to a variety of biological research fields by filling the gap between monolayers and animal models. The modern optical sectioning microscopic methods make it possible to probe the complexity of 3D cell cultures but are limited by the inherent opaqueness. While tissue optical clearing methods have emerged as powerful tools for investigating whole-mount tissues in 3D, they often have limitations, such as being too harsh for fragile 3D cell cultures, requiring complex handling protocols, or inducing tissue deformation with shrinkage or expansion. To address this issue, we proposed a modified optical clearing method for 3D cell cultures, called MACS-W, which is simple, highly efficient, and morphology-preserving. In our evaluation of MACS-W, we found that it exhibits excellent clearing capability in just 10 min,

[‖]Corresponding author.

with minimal deformation, and helps drug evaluation on tumor spheroids. In summary, MACS-W is a fast, minimally-deformative and fluorescence compatible clearing method that has the potential to be widely used in the studies of 3D cell cultures.

Keywords: Tissue optical clearing; 3D cell cultures; imaging.

1. Introduction

Three-dimensional (3D) cell cultures, such as spheroids or organoids, have become essential models for a broad range of biological research, including tumor biology, disease modeling and drug screening.[1–3] They can better mimic the features of *in vivo* microenvironments by re-establishing physiological cell–cell and cell–extracellular matrix (ECM)–cell interactions,[4] while avoiding the ethical issues and species-specific differences and ethical problems associated with animal models.

Modern optical imaging techniques, such as confocal or two-photon microscopy, have greatly contributed to 3D observation, which is crucial for obtaining accurate structural information of 3D cell cultures.[5–8] However, their intrinsic opaqueness of the multicellular structures limits light penetration, leading to unsatisfactory optical imaging performance in deeper layers.[9,10]

Tissue optical clearing techniques have been introduced to address this issue by reducing the scattering and absorption via physical and chemical strategies. Although most clearing protocols were developed or optimized for real tissues, various clearing methods have been implemented in the characterization of 3D cell cultures.[11] The hydrophobic methodologies, such as 3DISCO and Ethanol-ECi, have strong clearing capability and have been applied to retinal organoids,[12,13] and brain organoids,[14] but they are characterized by tissue shrinkage, potential fluorescence quenching, and toxicity. The hydrophilic clearing methodologies are most widely used in 3D cell cultures due to their ease of handling and safety. For instance, the CUBIC-series protocols have been used in tumor cell spheroids and ureteric bud organoids, and cortico-striatal assembloids.[15–17] But require multi-steps and are slow even when applied to small samples. The fructose-glycerol (FG) clearing agent enables high-resolution 3D imaging of human colonic organoids, but it causes organoid shrinkage which would alter the spherical shape of tissues with large lumens,[18] as like 88% Glycerol.[19] $Clear^{T2}$ has also been utilized to clear the HFIB spheroids and MCF-7 spheroids.[20] Some researchers also introduced hydrogel-based methods, such as CLARITY and SHIELD, into structural analysis of tumor cell spheroids or cerebral organoids[16,21]; although they have been combined with microfluidics to accelerate the process to achieve clearing within 5 h, this approach requires complicated chip design due to the complicated clearing protocol.[22] Moreover, the small and fragile nature of 3D cultures makes them susceptible to damage or loss during multi-step medium exchange operations. Therefore, single-step methods are preferred in clearing 3D cell cultures. A simple, highly efficient, and morphology-preserving method suitable for 3D cell cultures is thus needed. Emerging clearing agents, such as MACS(MXDA-based aqueous clearing system)-R1,[23] Ub-1,[24] and FOCM,[25] have been reported to perform excellently as rapid hydrophilic clearing agents for tissue slices or sections, showing great potential to be used in millimeter-scale 3D cell cultures.

In this work, we proposed a modified clearing solution for simple and rapid clearing of 3D spheroids, named MACS-W. MACS-W achieves higher transparency of 3D cell cultures than other methods with a simple one-step protocol in merely 10 min while maintaining ideal fluorescence compatibility and minimizing sample deformation. Furthermore, MACS-W enables 3D imaging of intact tumor spheroids and helps drug evaluation with more accurate quantitative analysis. We anticipate that MACS-W will be leveraged widely in broad biology research and drug discovery, potentially paving the way for new discoveries in the study of 3D cell cultures.

2. Materials & Methods

2.1. *Cell culture and spheroid formation*

HCT-116 (ATCC) cell line expressing GFP endogenously was cultured in RPMI 1640 medium (Gibco, C11875500BT) supplemented with 10% fetal bovine serum (FBS) and 1% penicillin-streptomycin in a humidified incubator (Thermo

Scientific, USA). When cells were grown to about 80% confluence, they were digested with trypsin-EDTA and resuspended in the medium. After pretreatment of the *U*-shaped 48-well plate with Anti-Adherence Solution (STEMCELL, 07010), spheroid production was initialized by seeding 10,000 cells per well. After that, the plate was centrifuged at 500 rpm for 5 min at room temperature. The medium was renewed every 2 days.

Each tumor spheroid was first rinsed thrice with PBS, and then treated with PFA (4% (w/v)) at 4°C overnight, followed by PBS rinse thrice for the following experiments.

2.2. *Clearing*

MACS-R0: MACS-R0 is a mixture of 20 vol% MXDA (Tokyo chemical industry, D0127) and 15% (w/v) sorbitol (Sigma-Aldrich, 85529) with ddH_2O. Tumor spheroids were incubated for 30 min.

MACS-R1: As described in the original literature, MACS-R1 can render 1-mm-thick brain sections cleared within 30 min.[23] Tumor spheroids were incubated in a mixture of 40 vol% MXDA and 30% (w/v) sorbitol with PBS (Sigma-Aldrich, P3813) for 30 min.

MACS-R2: MACS-R2 is a mixture of 40 vol% MXDA and 50% (w/v) sorbitol with ddH_2O. Tumor spheroids were incubated for 30 min.

MACS-W: Tumor spheroids were incubated in a mixture of 40 vol% MXDA and 30% (w/v) sorbitol with ddH_2O for 10 min.

88% Glycerol: Tumor spheroids were incubated in 88% glycerol (Sigma-Aldrich, V900860) prepared with ddH_2O for 1 h.

Ub-1: Ub-1 was prepared as a mixture of 25 wt% Meglumine (Shanghai Macklin Biochemical Co., M813277), 25 wt% Urea (Sigma-Aldrich, 15604), 20 wt% 1,3-Dimethyl-2-imidazolidinone (Sigma-Aldrich, 40727), and 0.2 wt% Triton X-100 (Sigma-Aldrich, T8787). The spheroids were incubated for 1 h.

FOCM: Tumor spheroids were incubated in DMSO (Sigma-Aldrich, D2650) solution containing 20% urea (Sigma-Aldrich, 15604), 30% sorbitol and 5% glycerol for 5 min.

The Osmotic pressure was measured using a Gonotec-3000 osmometer (Gonotec, Germany). The refractive indices were measured at about 20°C using an Abbe refractometer (WYA, Shanghai Yidian Physical Optics Instrument Co., Ltd., China).

2.3. *Staining*

Chemical Dye Staining: Two chemical dyes were used in this study. The PI powder (Beyotime Biotechnology, ST511) was dissolved in ethanol and diluted into the ddH_2O at a concentration of 5 μg/mL as working solution. The DiI (Beyotime Biotechnology, C1991S) working solution was obtained by mixing the DiI mother liquor and PBS at a rate of 1:1000. The spheroids were treated with each working solution overnight, and rinsed twice with 0.01 M PBS for 10 min.

Immunostaining: The following primary antibodies were used in this study: anti-Ki67 (Abcam, 1:200, ab279653), anti-Cas3 (Cell Signaling Technology, 1:400, 9661). Secondary antibodies including Alexa Fluor 405 (Abcam, 1:500, ab175660) and Alexa Fluor 594 (Abcam, 1:500, ab150080) were used. The fixed tumor spheroids were firstly blocked in 200 μL 0.2% PBST (0.2 vol% Triton X-100 in PBS) containing 10% goat serum (Boster Biological Technology, AR1009) overnight, and then subjected to immunostaining with 200 μL primary antibodies in 0.2% PBST containing 5% goat serum overnight. The spheroids were then rinsed with 0.2% PBST six times and immersed in 200 μL secondary antibodies in 0.2% PBST containing 5% goat serum for 6 h. The staining was conducted at room temperature on a shaker at 60 rpm. The samples were finally washed with 0.2% PBST six times and stored in PBS at 4°C prior to clearing.

2.4. *Drug treatment*

Apatinib (Beyotime Biotechnology, SF5454) was dissolved by DMSO and diluted into the medium at concentrations of 0, 5, 10 and 20 μM, then was introduced to the spheroids. After incubation at 37°C for 72 h, the spheroids were harvested and rinsed twice with 0.01 M PBS for 10 min each time.

2.5. *Imaging*

A Zeiss Axio Zoom.V16 microscope was used to acquire the wide-field images of the tumor spheroids before and after clearing.

Fluorescence images of tumor spheroids were obtained using a Zeiss confocal fluorescence microscope (Zeiss, LSM710, Germany) with Zen 2011 SP2 (V8.0.0.273, Zeiss, Germany) software. The samples were placed in a confocal dish, a Zeiss 10× Fluar objective (N.A. 0.5; air) was used for imaging.

2.6. *Data analysis*

All raw image data were acquired in CZI format and exported into TIFF format, MATLAB (v.2019a, Mathworks, USA) was used for image preprocessing. Imaris software was used to reconstruct image stacks and calculate the cell density in Fig. 4.

The transmittance performance in Fig. 1 is defined as the ratio of the pixel value of the sample to the pixel value of the background. The deformation of the tumor spheroid was defined by the change of the area of the corresponding fluorescence images before and after clearing, and was quantified with MATLAB.

The mean fluorescence intensity in Fig. 3 was the average intensity of the pixels in the spheroid images. The image contrast in Fig. 3 was defined as

$$C = \sqrt{\frac{\Sigma(I - I_m)^2}{n-1}}. \quad (1)$$

The imaging depth was defined as the z-depth where maximum mean fluorescence intensity was observed after clearing by the pre-clearing value.

Statistical analyses were performed using GraphPad Prism 8 (GraphPad Software, USA). All numerical data are presented as mean ± standard deviation (S.D.). In this study, p values were calculated using paired t test, and $p < 0.05$ was considered significant (n.s., not significant; *, $p < 0.05$; **, $p < 0.01$).

3. Results

3.1. *MACS-W is a rapid and morphology-preserving clearing method for 3D cell cultures*

As previously mentioned, acquiring the 3D structures of 3D cell cultures is crucial, and optical imaging methods have proven to be effective tools. However, the mismatch of the refractive index between the sample and the imaging medium limits the imaging performance.[10] Although numerous optical clearing methods have been developed, the majority of them are proposed for real tissues and may be time-consuming, labor-intensive, and result in sample deformation when applied to 3D cultures.

In this work, we initially compared several existing single-step clearing agents, including MACS-R0, MACS-R1, MACS-R2, 88% Glycerol, Ub-1 and FOCM, which showed big potential in the rapid and high-efficient clearing of small volumes. As the refractive index and the osmotic pressure are crucial factors for optical tissue clearing, we measured both parameters for all tested clearing agents (Figs. 1(a)–1(b)). We identified MACS-R1 to be an ideal candidate due to its high refractive index and low osmotic pressure, both of which are advantageous for achieving high transparency and low sample deformation. As shown in Figs. 1(c)–1(n), MACS-R1 achieved ideal transparency of tumor spheroids with a relatively small size deformation.

To address the shrinkage issue of MACS-R1, we tried to modify its agent content. Reducing the osmotic pressure should be an effective method. To ensure the clearing performance, we modified its agent content by replacing the PBS with water for a newly developed clearing agent, MACS-W. MACS-W exhibits the high transparency and excellent size maintenance capability while maintaining good clearing performance, making it an effective solution for clearing 3D cell cultures.

3.2. *MACS-W is compatible with various fluorescent probes*

Labeling plays a critical role in obtaining 3D structures of cell cultures. While the fluorescence compatibility of MACS with various dyes has been evaluated on real tissues, differences in operation procedure and sample type can affect overall compatibility. Besides, changes in ion concentration in MACS-W can also affect the fluorescence.[26] Thus, we performed an investigation into the fluorescence compatibility of MACS-W with several commonly-used fluorescent probes, including endogenous fluorescence protein, chemical dyes, and fluorophore-conjugated antibodies used in immunostaining. Confocal images of HCT-116 spheroids at a depth of 50 μm were obtained, and the representative results showed that all tested fluorescence probes were successfully preserved after clearing.

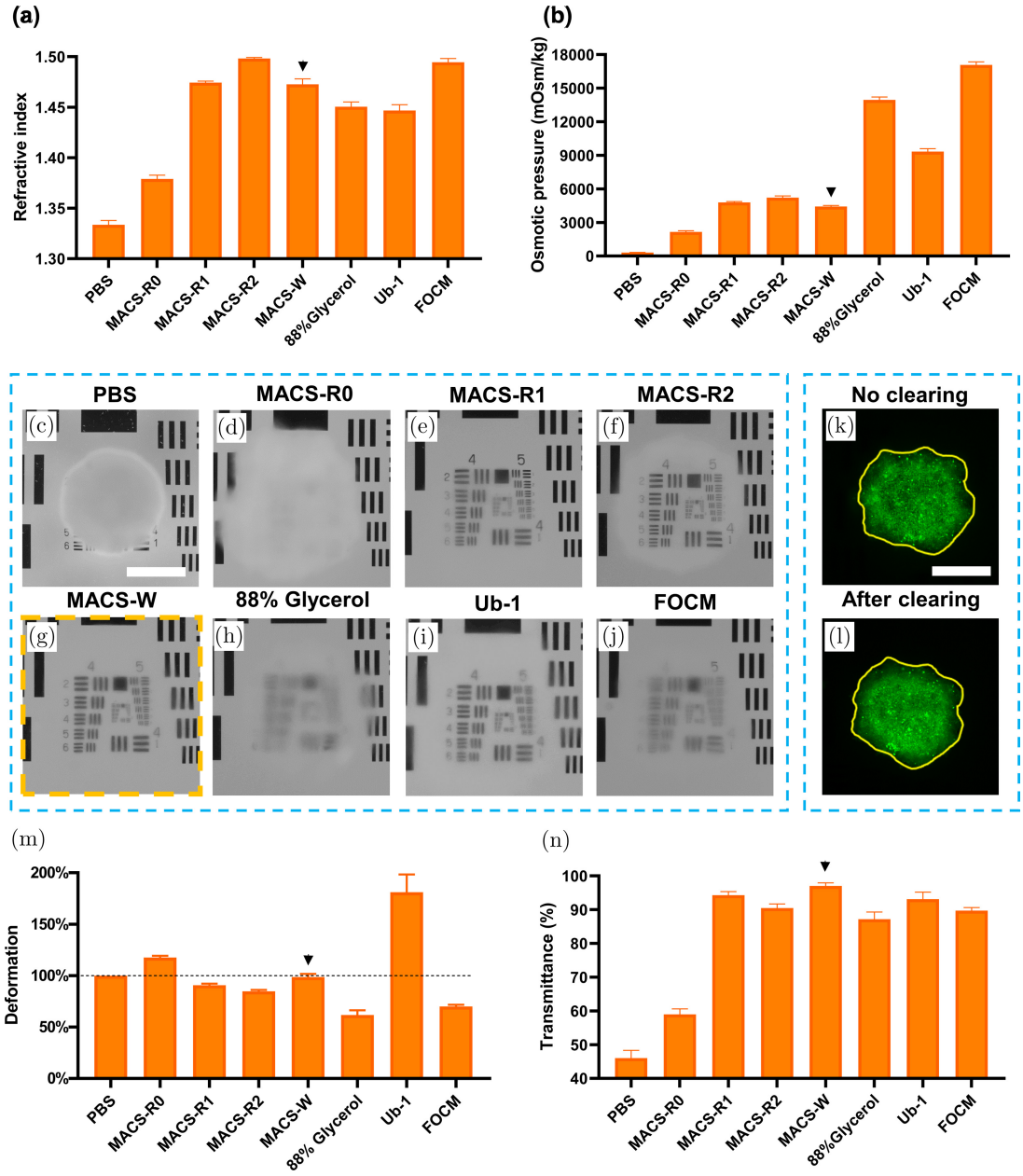

Fig. 1. Clearing performance of different clearing methods. (a), (b) Refractive index and osmotic pressure of different agents. (c)–(j) The bright-field images of HCT-116 tumor spheroids treated with different agents, scale bar: 400 μm. (k), (l) Illustration of size quantification of size changes based on fluorescence image, scale bar: 400 μm. The yellow lines indicate the outlines of the samples. (m) Quantified size changes. (n) Transmittance. ($n = 3$ for (a), (b), (m); $n = 4$ for (n)).

These results demonstrate the potential of MACS-W for use in multicolor imaging in future applications (Fig. 2).

3.3. *MACS-W increases fluorescence imaging performance*

To evaluate the enhancement of imaging performance provided by MACS-W, we utilized GFP as an example and imaged the same HCT-116 tumor spheroids using confocal microscopy before and after clearing. The resulting images acquired at various depths are presented in Fig. 3(a). Enlarged views showed that MACS-W improved image quality in deeper layers, as evident in Fig. 3(b). Additionally, the orthogonal projection (x–z projection) exhibited a noticeably increased imaging depth by 66.7% (Fig. 3(c)). Furthermore, we

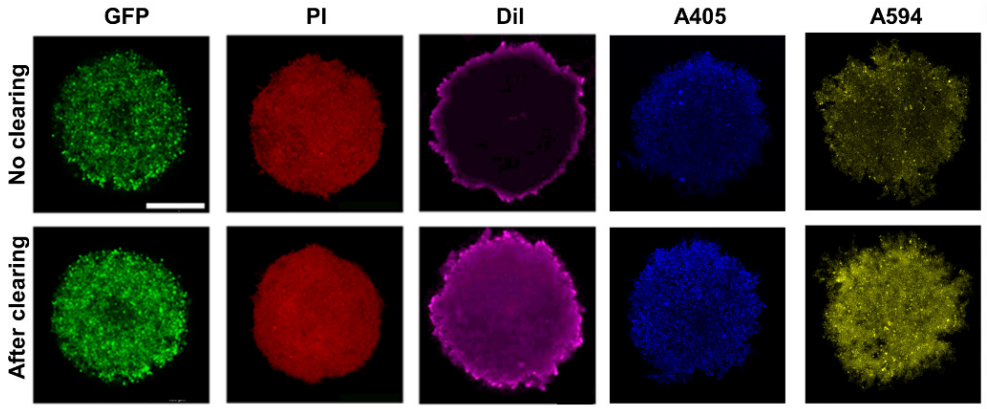

Fig. 2. Fluorescence compatibility of commonly used fluorescent probes with MACS-W, including GFP, PI, DiI, Alexa Fluor 405 and Alexa Fluor 594, depth: 50 μm, scale bar: 400 μm.

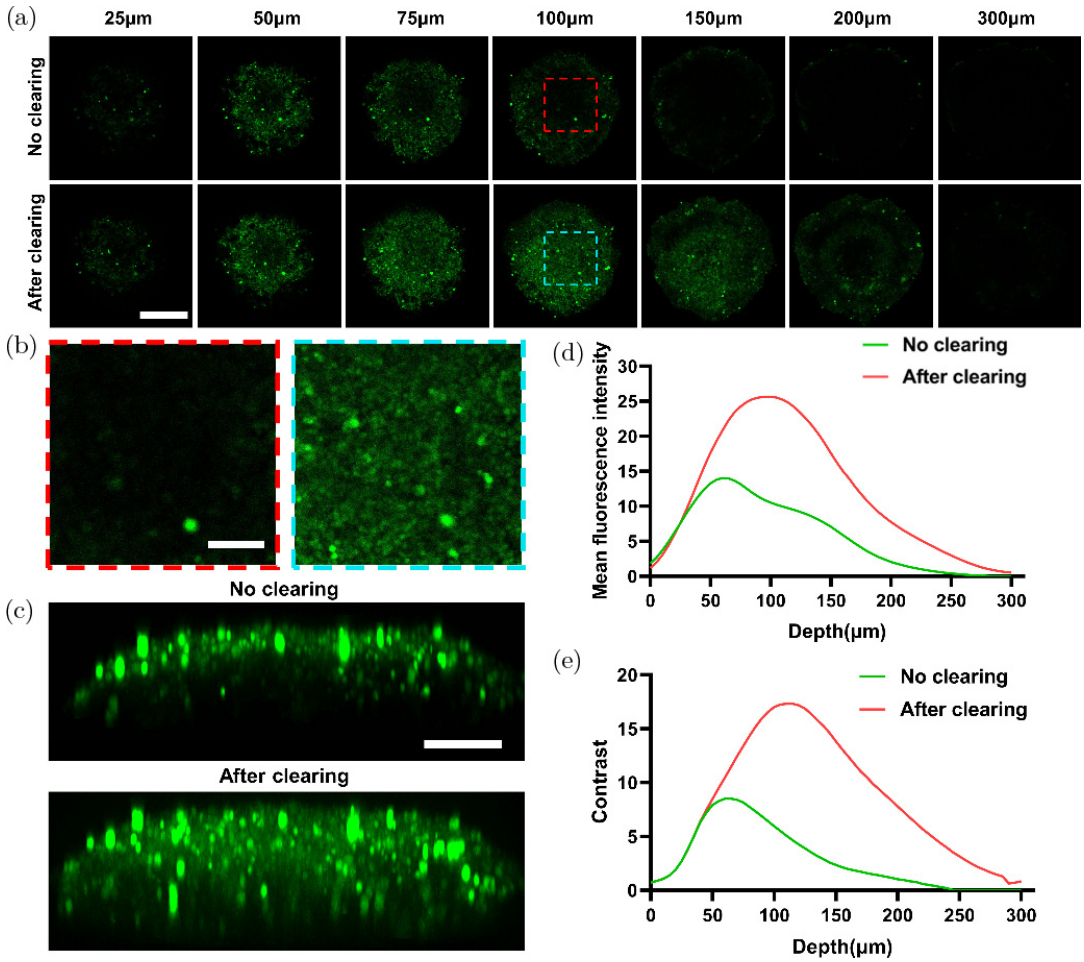

Fig. 3. MACS-W increases the imaging performance. (a) Fluorescence images of HCT-116 spheroids at different depths before and after clearing, scale bar: 400 μm. (b) Enlarged view of the regions boxed with the dashed rectangle in (a), scale bar, 50 μm. (c) Orthogonal view (x–z) of the image stacks, scale bar: 200 μm. (d) Represented curves of mean fluorescence intensity against z-depth. (e) Represented curves of contrast against z-depth.

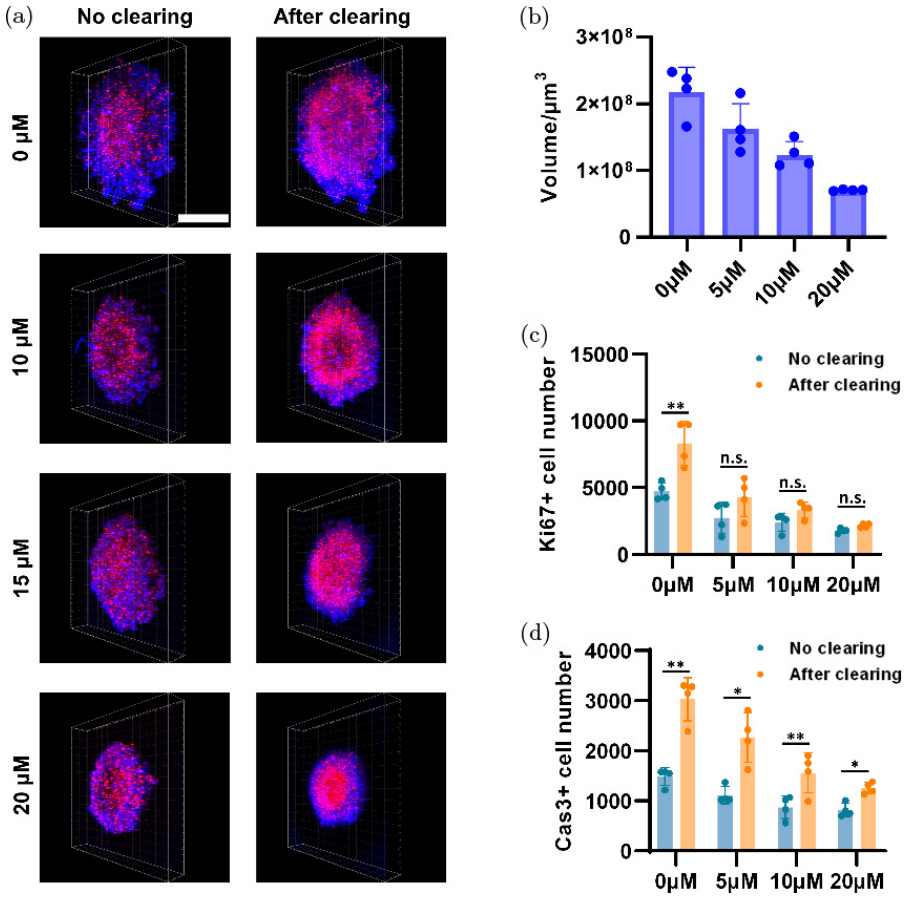

Fig. 4. MACS-W helps drug evaluation. (a) Represented fluorescence images of HCT-116 tumor spheroids after 72 h drug treatment in varied doses, Scale bar: 500 μm. (b) Volume of spheroids treated with different doses. (c) Total number of proliferating cells (Ki67+) at each dose. (d) Total number of Cas3+ cells at each dose. The values are the mean ± S.D.; statistical significance (n. s., not significant; *, $p < 0.05$; **, $p < 0.01$) was assessed by paired t test, $n = 4$.

calculated both the mean fluorescence intensity and contrast across the z-depth of the sample (Figs. 3(d) and 3(e)). These quantitative results demonstrated that MACS-W enhances imaging performance in deeper layers, allowing for observation of previously inaccessible regions.

3.4. *MACS-W helps drug evaluation*

Apatinib is a small-molecule antiangiogenic agent that has been shown to induce protective autophagy in cancer cells through endoplasmic reticulum stress.[27] Additionally, studies have suggested that Apatinib can enhance apoptosis in HCT-116 cells.[27,28] To further assess the effectiveness of Apatinib, we applied MACS-W to HCT-116 spheroids for drug evaluation.

We treated the tumor spheroids with varying doses of Apatinib and imaged the spheroids using confocal fluorescence microscopy before and after clearing, generating 3D structures (Fig. 4(a)). Figure 4(b) demonstrates that the spheroid size decreased with increasing Apatinib concentration. We also counted the number of proliferating cells (Ki67+) and apoptotic cells (Cas3+) before and after clearing. The results shown in Figs. 4(c) and 4(d) indicate that the MACS-W significantly increased the cell counting accuracy and enhanced the difference in cell counts between the various drug doses. Overall, these findings illustrate the potential effectiveness of MACS-W in drug evaluation studies, particularly for the evaluation of antiangiogenic agents like Apatinib.

4. Discussion

In this study, we described a modified clearing agent for 3D cell cultures, termed MACS-W. This work of

MACS-W lies in its ability to maintain the size of 3D cell cultures without causing sample deformation, a common problem observed in existing methods such as MACS-R1. We achieved this by adjusting the reagent of MACS-R1. Benefitting from the high-speed performance of MACS-R1, MACS-W offers rapid and minimally-deformative processing, enabling for the acquisition of high-resolution 3D structures of tumor spheroids.

As a rapid aqueous clearing protocol for whole organs, MACS involves a tri-step protocol with graded chemical solutions, including MACS-R0, MACS-R1, and MACS-R2. For the tissue sections, MACS-R1 was used in original paper.[23] We speculate that the shrinkage induced by MACS-R1 and MACS-R2 is partially due to the high osmotic pressure. MACS-R1 is composed of three components: MXDA, sorbitol, and PBS, while MACS-R2 is composed of MXDA, sorbitol, and ddH_2O. To ensure clearing performance, the concentration of MXDA and sorbitol has already been finely tuned. Therefore, a feasible approach is to adjust the water and PBS. Since introducing any solute into water will increase the osmotic pressure, we modified MACS-R1 by replacing the PBS with ddH_2O and described MACS-W for size maintenance of tumor spheroids.[23] For 3D cultures with cavity structures, such as intestinal organoids and cardioids mentioned before, these cavity structures often bear some structural functions, so it is extremely important to maintain the morphology of the samples during the clearing process. MACS-W can handle this task well and is expected to play an important role in 3D cultures research. In regard to the comparison of fluorescence imaging effects with other clearing methods, we excluded the reference methods after evaluating clearing performance based on transparency and size maintenance. Therefore, we only assessed the imaging capability of MACS-W. Moreover, we believe that assessing tissue transparency and fluorescence compatibility should provide adequate information regarding performance, obviating the need for direct comparison of imaging depth between different methods. Additionally, it is important to note that tissue shrinkage induced by most reference methodologies can cause reduced imaging depth, which may result in unfair comparisons and inaccurate evaluations of other reference methods.

For the particular application in 3D cell cultures, the usage of existing clearing protocols for real tissues is a viable approach. In principle, it should be much simpler to render 3D cell cultures transparent. However, due to the differences between 3D cell cultures and real tissues,[29] methods developed for real tissues may not perform well on 3D cell cultures. This necessitates meticulous optimization of the clearing step, reagent's concentration, type and treatment environment of the original method. In addition, due to their small and fragile nature, 3D cultures are difficult to manipulate, and multiple steps in the methods may lead to sample loss or damage. Therefore, special equipment, such as microfluidics, was required. While the design of microfluidic chips and fluid control equipment can pose a threshold for researchers (specifically operators), the integrated nature of the chips often enables high-throughput organoid detection with simple operations. As a result, microfluidic chips have been widely applied in developing and clearing 3D cell cultures,[22,30–34] while some chips were designed with complexity to match the complicated clearing protocols,[22,33] such as hydrogel-embedding methods, an efficient single-step clearing method would simplify the integration of a simple chip design with the clearing process. Combined with the microfluidics, MACS-W is expected to realize the integrated process of the culture, clearing, staining, and imaging in one chip, showing great potential in high-throughput analysis of spheroids or organoids in the future.

HCT-116 spheroids are a simple and typical 3D cell culture that possess the basic characteristics of a 3D tumor model while also being low in cost and easy to cultivate. Therefore, they were selected as the experimental model for this study. While the research focused specifically on tumor spheroids, the potential of MACS-W in other 3D cell cultures cannot be ruled out. For example, cardioids[35,36] and brainoids[37] are also complex 3D tissue models that have been used in organ development and brain disease research. However, achieving high-resolution and intuitive imaging results in these models has been challenging due to the high scattering in cardioids and the need for accurate 3D descriptions in brainoids. Although MACS-W shows great potential for small 3D cell cultures, its clearing efficiency for larger samples requires further investigation. In the future, a more efficient clearing protocol for a broad range of 3D cultures can be developed through fine screening of different reagents.

Tumor spheroids, like real tumors, have a complex, multi-layered structure with cells in the core and periphery exhibiting different behaviors.[38] Due to limited nutrition, the cells in the core of tumor spheroids may undergo apoptosis, while those in the periphery tend to proliferate more actively.[39] In our study, we did not observe a significant difference in proliferating cell counting before and after clearing at 20 μM. This could be attributed to the fact that proliferating cells are distributed more in the easily-imaged periphery. However, we did observe a significant difference in apoptotic cell counting for all doses, which may be due to the higher concentration of apoptotic cells in the core of the spheroids. Unfortunately, the strong scattering in the core region made imaging difficult prior to clearing, highlighting the value of this technique in improving our ability to study complex tissue structures.

5. Conclusions

In conclusion, MACS-W is an optimized optical clearing agent for 3D cell cultures. By addressing the unique challenges associated with clearing 3D cell cultures, MACS-W offers a rapid, minimally-deformative, and fluorescence compatible solution that enables high-resolution imaging of 3D structures. As such, MACS-W is poised to make significant contributions to fundamental research, drug development, and disease treatment by offering researchers the ability to better visualize and quantify the behavior of cells in 3D contexts. As such, MACS-W represents a critical tool for advancing our understanding of complex biological systems.

Acknowledgments

We thank the support from the National Key Research and Development Program of China (Grant No. 2017YFA0700501), and the Innovation Fund of WNLO. We also thank the Optical Bio-imaging Core Facility of WNLO-HUST for their assistance with data acquisition.

Conflicts of Interest

The authors declare no conflicts of interest.

References

1. T. A. V. Afanasyeva, J. C. Corral-Serrano, A. Garanto, R. Roepman, M. E. Cheetham, R. W. J. Collin, "A look into retinal organoids: Methods, analytical techniques, and applications," *Cell. Mol. Life Sci.* **78**, 6505–6532 (2021).
2. H. Xu, X. Lyu, M. Yi, W. Zhao, Y. Song, K. Wu, "Organoid technology and applications in cancer research," *J. Hematol. Oncol.* **11**, 116 (2018).
3. B. Cunniff, J. E. Druso, J. L. van der Velden, "Lung organoids: Advances in generation and 3D-visualization," *Histochem. Cell Biol.* **155**, 301–308 (2021).
4. J. Friedrich, C. Seidel, R. Ebner, L. A. Kunz-Schughart, "Spheroid-based drug screen: Considerations and practical approach," *Nat. Protocols* **4**, 309–324 (2009).
5. M. R. Blatchley, K. A. Gunay, F. M. Yavitt, E. M. Hawat, P. J. Dempsey, K. S. Anseth, "*In situ* super-resolution imaging of organoids and extracellular matrix interactions via phototransfer by allyl sulfide exchange-expansion microscopy (PhASE-ExM)," *Adv. Mater.* **34**, e2109252 (2022).
6. E. C. Costa, A. F. Moreira, D. de Melo-Diogo, I. J. Correia, "ClearT immersion optical clearing method for intact 3D spheroids imaging through confocal laser scanning microscopy," *Opt. Laser Technol.* **106**, 94–99 (2018).
7. E. C. Costa, D. N. Silva, A. F. Moreira, I. J. Correia, "Optical clearing methods: An overview of the techniques used for the imaging of 3D spheroids," *Biotechnol. Bioeng.* **116**, 2742–2763 (2019).
8. Q. Huang, A. Garrett, S. Bose, S. Blocker, A. C. Rios, H. Clevers, X. Shen, "The frontier of live tissue imaging across space and time," *Cell Stem Cell* **28**, 603–622 (2021).
9. T. Tian, Z. Yang, X. Li, "Tissue clearing technique: Recent progress and biomedical applications," *J. Anat.* **238**, 489–507 (2020).
10. V. Tuchin, I. Maksimova, D. Zimnyakov, I. Kon, A. Mavlyutov, A. Mishin, "Light propagation in tissues with controlled optical properties," *J. Biomed. Opt.* **2**, 401–417 (1997).
11. E. A. Susaki, M. Takasato, "Perspective: Extending the utility of three-dimensional organoids by tissue clearing technologies," *Front. Cell. Dev. Biol.* **9**, 679226 (2021).
12. M. Garita-Hernandez, L. Guibbal, L. Toualbi, F. Routet, A. Chaffiol, C. Winckler, M. Harinquet, C. Robert, S. Fouquet, S. Bellow, J. A. Sahel, O. Goureau, J. Duebel, D. Dalkara, "Optogenetic light sensors in human retinal organoids," *Front. Neurosci.* **12**, 789 (2018).
13. H. Renner, M. Grabos, K. J. Becker, T. E. Kagermeier, J. Wu, M. Otto, S. Peischard, D. Zeuschner, Y. TsyTsyura, P. Disse, J. Klingauf, S. A. Leidel, G. Seebohm, H. R. Schöler, J. M. Bruder, "A fully automated high-throughput workflow for 3D-based

chemical screening in human midbrain organoids," *eLife* **9**, e52904 (2020).
14. G. Goranci-Buzhala, A. Mariappan, E. Gabriel, A. Ramani, L. Ricci-Vitiani, M. Buccarelli, Q. G. D'Alessandris, R. Pallini, J. Gopalakrishnan, "Rapid and efficient invasion assay of glioblastoma in human brain organoids," *Cell Rep.* **31**, 107738 (2020).
15. S. I. Mae, M. Ryosaka, S. Sakamoto, K. Matsuse, A. Nozaki, M. Igami, R. Kabai, A. Watanabe, K. Osafune, "Expansion of human iPSC-derived ureteric bud organoids with repeated branching potential," *Cell Rep.* **32**, 107963 (2020).
16. A. Masson, P. Escande, C. Frongia, G. Clouvel, B. Ducommun, C. Lorenzo, "High-resolution in-depth imaging of optically cleared thick samples using an adaptive SPIM," *Sci. Rep.* **5**, 16898 (2015).
17. Y. Miura, M. Y. Li, O. Revah, S. J. Yoon, G. Narazaki, S. P. Pasca, "Engineering brain assembloids to interrogate human neural circuits," *Nat. Protocols* **17**, 15–35 (2022).
18. J. F. Dekkers, M. Alieva, L. M. Wellens, H. C. R. Ariese, P. R. Jamieson, A. M. Vonk, G. D. Amatngalim, H. Hu, K. C. Oost, H. J. G. Snippert, J. M. Beekman, E. J. Wehrens, J. E. Visvader, H. Clevers, A. C. Rios, "High-resolution 3D imaging of fixed and cleared organoids," *Nat. Protocols* **14**, 1756–1771 (2019).
19. E. Steinberg, N. Orehov, K. Tischenko, O. Schwob, G. Zamir, A. Hubert, Z. Manevitch, O. Benny, "Rapid clearing for high resolution 3D imaging of *ex vivo* pancreatic cancer spheroids," *Int. J. Mol. Sci.* **21**, 7703 (2020).
20. E. C. Costa, A. F. Moreira, D. de Melo-Diogo, I. Correia, "Polyethylene glycol molecular weight influences the ClearT2 optical clearing method for spheroids imaging by confocal laser scanning microscopy," *J. Biomed. Opt.* **23**, 1–11 (2018).
21. A. Albanese, J. M. Swaney, D. H. Yun, N. B. Evans, J. M. Antonucci, S. Velasco, C. H. Sohn, P. Arlotta, L. Gehrke, K. Chung, "Multiscale 3D phenotyping of human cerebral organoids," *Sci. Rep.* **10**, 21487 (2020).
22. T. Silva Santisteban, O. Rabajania, I. Kalinina, S. Robinson, M. Meier, "Rapid spheroid clearing on a microfluidic chip," *Lab Chip* **18**, 153–161 (2017).
23. J. Zhu, T. Yu, Y. Li, J. Xu, Y. Qi, Y. Yao, Y. Ma, P. Wan, Z. Chen, X. Li, H. Gong, Q. Luo, D. Zhu, "MACS: Rapid Aqueous Clearing System for 3D Mapping of Intact Organs," *Adv. Sci. (Weinh)* **7**, 1903185 (2020).
24. L. Chen, G. Li, Y. Li, Y. Li, H. Zhu, L. Tang, P. French, J. McGinty, S. Ruan, "UbasM: An effective balanced optical clearing method for intact biomedical imaging," *Sci. Rep.* **7**, 12218 (2017).
25. X. Zhu, L. Huang, Y. Zheng, Y. Song, Q. Xu, J. Wang, K. Si, S. Duan, W. Gong, "Ultrafast optical clearing method for three-dimensional imaging with cellular resolution," *Proc. Natl. Acad. Sci. USA* **116**, 11480–11489 (2019).
26. R. K. Henderson, A. Baker, K. R. Murphy, A. Hambly, R. M. Stuetz, S. J. Khan, "Fluorescence as a potential monitoring tool for recycled water systems: A review," *Water Res.* **43**, 863–881 (2009).
27. Z. Zhang, F. Luo, Y. Zhang, Y. Ma, S. Hong, Y. Yang, W. Fang, Y. Huang, L. Zhang, H. Zhao, "The ACTIVE study protocol: Apatinib or placebo plus gefitinib as first-line treatment for patients with EGFR-mutant advanced non-small cell lung cancer (CTONG1706)," *Cancer Commun.* **39**, 69 (2019).
28. X. Tian, S. Li, G. Ge, "Apatinib promotes ferroptosis in colorectal cancer cells by targeting ELOVL6/ACSL4 signaling," *Cancer Manag. Res.* **13**, 1333–1342 (2021).
29. F. Pampaloni, E. G. Reynaud, E. H. Stelzer, "The third dimension bridges the gap between cell culture and live tissue," *Nat. Rev. Mol. Cell. Biol.* **8**, 839–845 (2007).
30. A. Cochrane, H. J. Albers, R. Passier, C. L. Mummery, A. van den Berg, V. V. Orlova, A. D. van der Meer, "Advanced in vitro models of vascular biology: Human induced pluripotent stem cells and organ-on-chip technology," *Adv. Drug Deliv. Rev.* **140**, 68–77 (2019).
31. B. Patra, Y. H. Chen, C. C. Peng, S. C. Lin, C. H. Lee, Y. C. Tung, "A microfluidic device for uniform-sized cell spheroids formation, culture, harvesting and flow cytometry analysis," *Biomicrofluidics* **7**, 54114 (2013).
32. P. Järvinen, A. Bonabi, V. Jokinen, T. Sikanen, "Simultaneous culturing of cell monolayers and spheroids on a single microfluidic device for bridging the gap between 2D and 3D cell assays in drug research," *Adv. Funct. Mater.* **30**, 2000479 (2020).
33. Y. Y. Chen, P. N. Silva, A. M. Syed, S. Sindhwani, J. V. Rocheleau, W. C. W. Chan, "Clarifying intact 3D tissues on a microfluidic chip for high-throughput structural analysis," *Proc. Natl. Acad. Sci. USA* **113**, 14915–14920 (2016).
34. X. J. Li, A. V. Valadez, P. Zuo, Z. Nie, "Microfluidic 3D cell culture: Potential application for tissue-based bioassays," *Bioanalysis* **4**, 1509–1525 (2012).
35. J. H. Park, J. Lee, S.-H. Park, K.-S. Kim, "Optimizing a three-dimensional spheroid clearing method for the imaging-based evaluation of cardiotoxicity," *Organoid* **1**, e7 (2021).
36. P. Hofbauer, S. M. Jahnel, N. Papai, M. Gieshammer, A. Deyett, C. Schmidt, M. Penc,

K. Tavernini, N. Grdseloff, C. Meledeth, L. C. Ginistrelli, C. Ctortecka, Š. Šalic, M. Novatchkova, S. Mendjan, "Cardioids reveal self-organizing principles of human cardiogenesis," *Cell* **184**, 3299–3317.e3222 (2021).

37. M. A. Lancaster, M. Renner, C.-A. Martin, D. Wenzel, L. S. Bicknell, M. E. Hurles, T. Homfray, J. M. Penninger, A. P. Jackson, J. A. Knoblich, "Cerebral organoids model human brain development and microcephaly," *Nature* **501**, 373–379 (2013).
38. S. J. Han, S. Kwon, K. S. Kim, "Challenges of applying multicellular tumor spheroids in preclinical phase," *Cancer Cell Int.* **21**, 152 (2021).
39. E. C. Costa, A. F. Moreira, D. de Melo-Diogo, V. M. Gaspar, M. P. Carvalho, I. J. Correia, "3D tumor spheroids: An overview on the tools and techniques used for their analysis," *Biotechnol. Adv.* **34**, 1427–1441 (2016).